

Sensor and Simulation Notes

Note 392

10 February 1996

Transient Arrays

Carl E. Baum
Phillips Laboratory

Abstract

Arrays for radiating large fast electromagnetic pulses are an outgrowth of nuclear EMP simulation technology. Here the question was how to launch TEM waves (planar or spherical) over large apertures (meters) with high voltages (megavolts) and fast risetimes (nanoseconds). In this case the aperture source distributions were made to match the appropriate TEM modal distributions (in general nonuniform) corresponding to cylindrical or conical transmission lines. Note that while the highest frequencies in the pulse restrict the size of individual elements of the array, it was recognized ab initio that the elements had to be connected together in a manner to pass low-frequency currents through the array and thereby produce the low-frequency portions of the pulse.

Large transient arrays were also considered in the same time frame for radiating unguided waves with otherwise similar parameters. Using unit cells based on interconnected conical transmission lines (TEM horns) various symmetries can be imposed on the array based on the two-dimensional space groups. Among the possibilities are unit cells based on squares, regular hexagons, and equilateral triangles.

In a more modern context transient arrays are being considered for applications in which sub nanosecond-risetime pulses are to be applied to the array elements to make an impulse radiating antenna (IRA) with performance similar to reflector IRAs and lens IRAs. The benefit to be gained (say for radar applications) is the ability to electronically steer the beam. However, this benefit is gained at the cost of greater complexity due to the large number of array elements and the requirement for accurate rapidly adjustable times for triggering the individual elements (sources). There is a significant trade off between the scan angle for the beam and the element size, risetime and angle between the TEM-horn conductors. In addition, as in the cases of other types of IRAs, an array IRA can be designed with auxiliary conductors and resistors to match the low frequency electric- and magnetic-dipole moments so as to give some desirable low-frequency directivity to the beam.

PL/PA 9 Apr 96
DL 96-0304

1. Introduction

Analogous to phased arrays with narrowband excitation one can have timed arrays for radiating transient pulses, the role of phase being replaced by the time shifts between the application of temporal waveforms (or one common waveform) to the various array elements. Our concern here is for such arrays to operate in transmission and/or reception over very large band ratios (ratio of upper frequency to lower frequency of interest), similar to other forms of impulse radiating antennas (IRAs) using reflectors or lenses [29, 30]. One might think of such transient arrays as array IRAs.

Such arrays are an extension of those studied, and in some cases realized, for simulation of the nuclear electromagnetic pulse (EMP) [13, 27]. Such an array has been referred to as a distributed source [3, 4] or a distributed switch [14]. In this case, the approach consists of synthesizing the TEM mode (planar or spherical, in general inhomogeneous) over some aperture surface serving as the electrical source for a cylindrical or conical transmission line. By use of such a technique one can suppress the generation of higher order (E and H) modes up to frequencies limited, not by wavelengths of the order of (or larger than) the transmission-line-conductor spacing and width, but by wavelengths of the order of (or larger than) the element spacing in the array forming the distributed source. The reader should note that such arrays are comprised of interconnected elements which allow for current continuity through the array, this being essential for adequate low-frequency performance. In contradistinction to the case of many narrow-band arrays in which the mutual interaction of the array elements is made (or assumed) small, the present arrays are designed so that the mutual interaction is strong and is an integral part of the array operation, at least for frequencies with wavelengths of the order of and larger than the element spacing.

The motivation for developing such arrays to drive EMP simulators has been the desire to go to higher and higher voltages while retaining a sufficiently small risetime in the pulse. As one goes to higher voltages (MV) on a single switch the risetime increases to the point where one considers using multiple switches at lower voltages. These switches then need to be distributed over an appropriate aperture to synthesize the desired TEM wave. Note that the risetime is influenced not only by the switch size, but also by how these switches are integrated into the array-element design, and how small is the jitter in the timing of these switches as compared to the ideal (desired) switching time.

An important approach to synthesis of a transient array is an array of flat-plate conical transmission lines each launching a spherical TEM wave from a small source, these waves combining on an aperture plane feeding a parallel-plate cylindrical (or conical) transmission line [1] illustrated in fig. 1. Some improvement in the aperture synthesis is obtained as the individual wave launchers are lengthened to

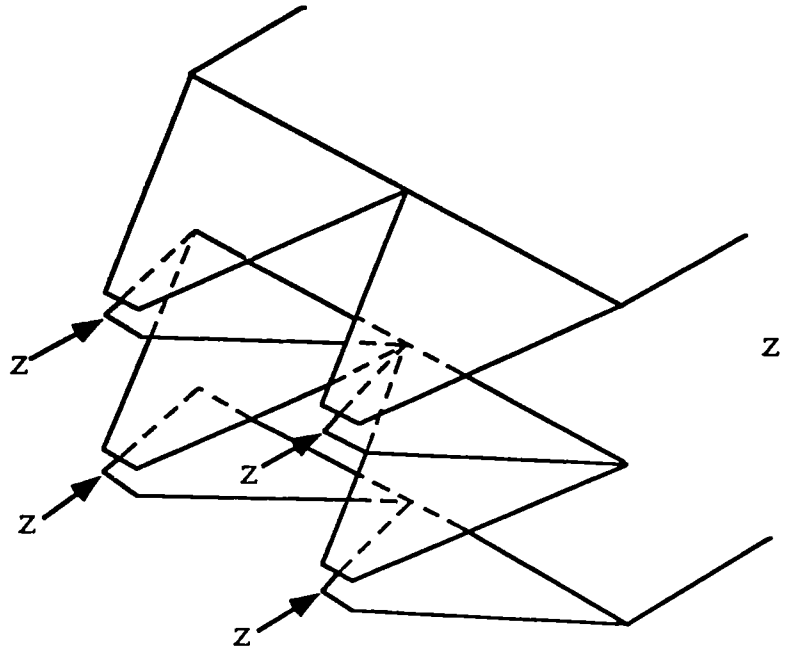


Fig. 1. Multiple Conical Transitions

make the spherical waves better approximate a plane wave on the aperture plane. One can have individual pulsers at the apices of the individual-element conical transmission lines, or one can feed various numbers of such source points from one or more common pulsers via transmission lines [1] as indicated by the example in fig. 2. Various combinations of series and parallel connections with appropriate matched delays (transit times in the transmission lines) are possible. Later papers [2-4, 6-10, 12-16, 23] have considered more details of such transient arrays in the context of EMP simulators.

Such arrays have been realized in EMP simulators. The large ATLAS I for testing large aircraft [13, 27] has a two-element array in a series configuration (fig. 1) with the two adjacent conical plates connecting at the aperture plane being larger than the two outermost so as to form a central-ground-plane wedge and prevent coupling between the two launchers until they meet at the aperture plane [1]. The SIEGE simulation concept [13] replaces one of the plates of a two-parallel-plate waveguide by the earth surface for testing buried systems. This has been realized using a four-parallel-element array in which the long conical plates are bent in a contour to account for mutual interaction before the aperture plane and thereby maintain a constant characteristic impedance along each of the four wave launchers [2]. Another type of simulator for buried systems is DISCUS [4, 13] in which the array is attached to the ground surface for driving the fields into the earth, thereby introducing additional matching problems at the ground surface. Such wave launchers have been designed and constructed involving Brewster-angle and transmission-line techniques [15, 23]. In one experiment a twelve-element array (100 kV pulser per element, dimensions 1 m in the direction of the electric field and 2 m in the direction of the magnetic field), connected in series with fiber-optic signals to trigger each pulser module, produced about 70 kV/m with 7 ns risetime in the soil [16].

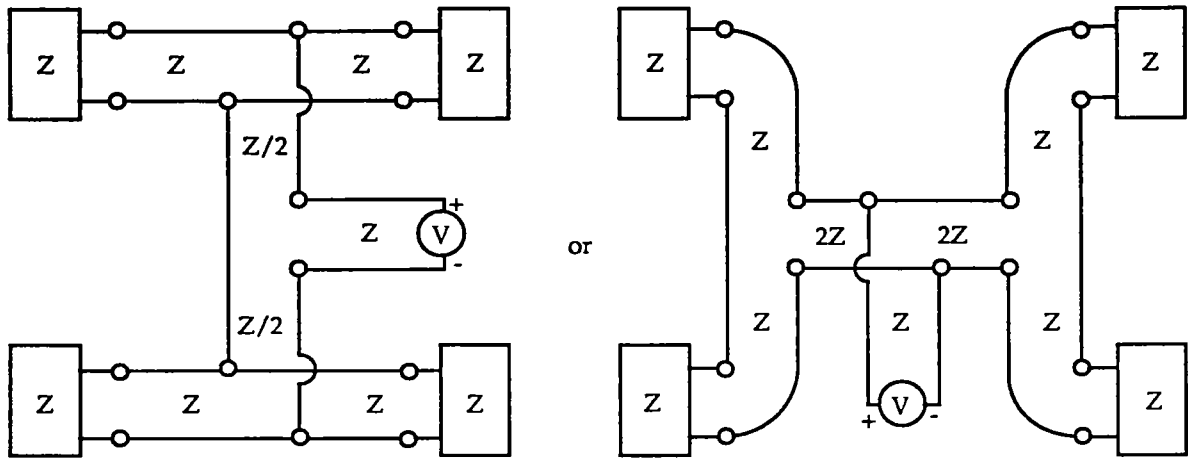


Fig. 2. Single Signal Feed Transmission Line Networks for Multiple Conical Feed Points

2. Early considerations for radiating transient arrays

There was early recognition [5] that such arrays were also suitable for radiating transient pulses, i.e., without an additional waveguiding structure (cylindrical or conical transmission line). In this case, the object was to see what kinds of pulses could be sent to distances far from the radiating source array using the kinds of pulse power technology in EMP simulators.

Approximating large arrays as infinite for initial considerations (theoretical simplification) one can pay attention to the details of the unit cells (individual elements) in an array of identical unit cells which is periodic in two dimensions. Thus one can have waves propagating in each cell, including interaction with other cells, without including effects associated with array truncation (edge effects). A section of such an array with rectangular unit cells [5] (height w_1 , width w_2) comprised of conical transmission lines is illustrated in fig. 3. This is but one of various types of unit cells that one might consider for array elements. The two-dimensional translation group T_2 admits five kinds of parallelogram systems for the boundaries of the unit cells [25, 31]. One can adjoin compatible rotations and reflections in the unit cells to give the two-dimensional space groups E_2 with a richer symmetry structure. Some of the more interesting types of unit cells are illustrated in fig. 4 based on squares, regular hexagons, and equilateral triangles [5]. In this case, the unit cells are configured such that by changing electrical connections to the sources one can achieve multiple polarizations.

The early-time (or, equivalently, high-frequency) performance of an infinite array of conical wave launchers can be found by first considering the same performance regime of a single conical element [11, 17]. As indicated in fig. 5 consider a rectangular array of elements with source points (conical apices) on the $z = 0$ plane. Letting one element have conical apex at $\vec{r} = \vec{0}$ with voltage excitation $V_0 u(t)$, the early-time field is described by the TEM field

$$\vec{E}(\vec{r}, t) = -\frac{V_0}{r} \vec{F}(\theta, \phi) u\left(t - \frac{r}{c}\right), \quad \vec{F}(\theta, \phi) = \nabla_{\theta, \phi} f(\theta, \phi) \quad (2.1)$$

where $f(\theta, \phi)$ is the potential function and $\nabla_{\theta, \phi}$ is the gradient on the unit sphere in the usual spherical coordinate system. The form that $f(\theta, \phi)$ takes depends on the detailed shape of the conical-transmission-line elements. Detailed calculations have been performed [11, 17] for planar bicones and flat-plate cones such as in fig. 3.

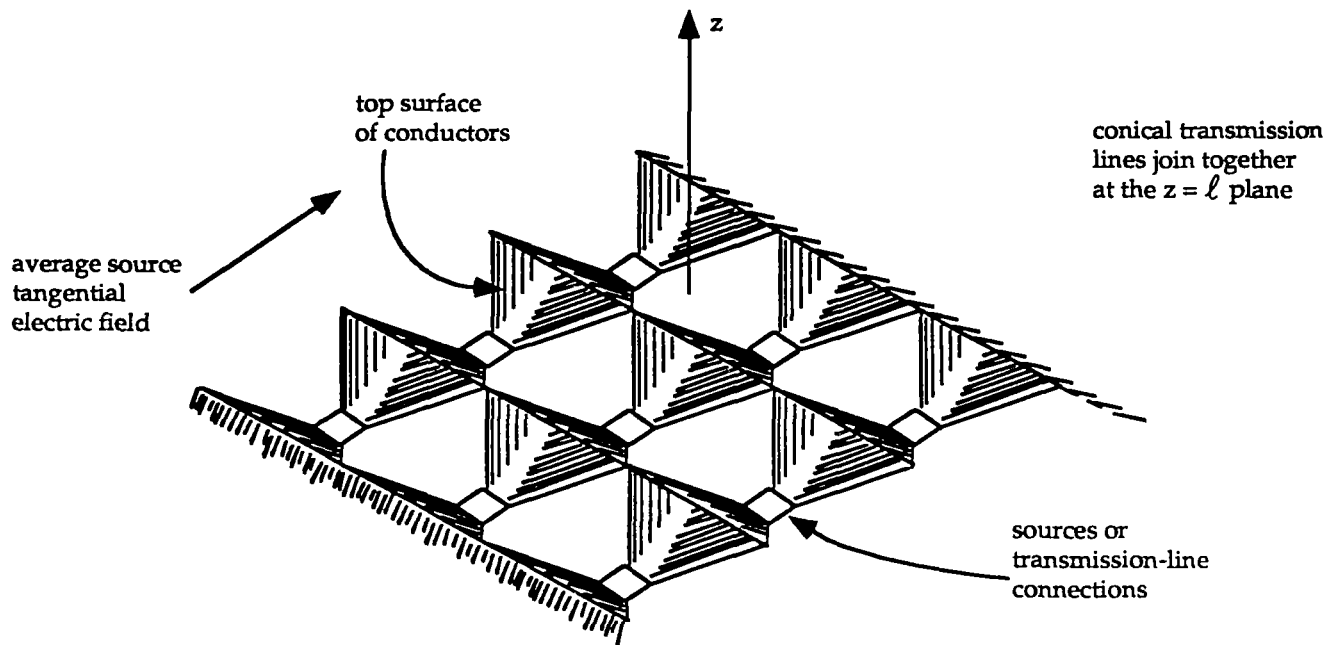
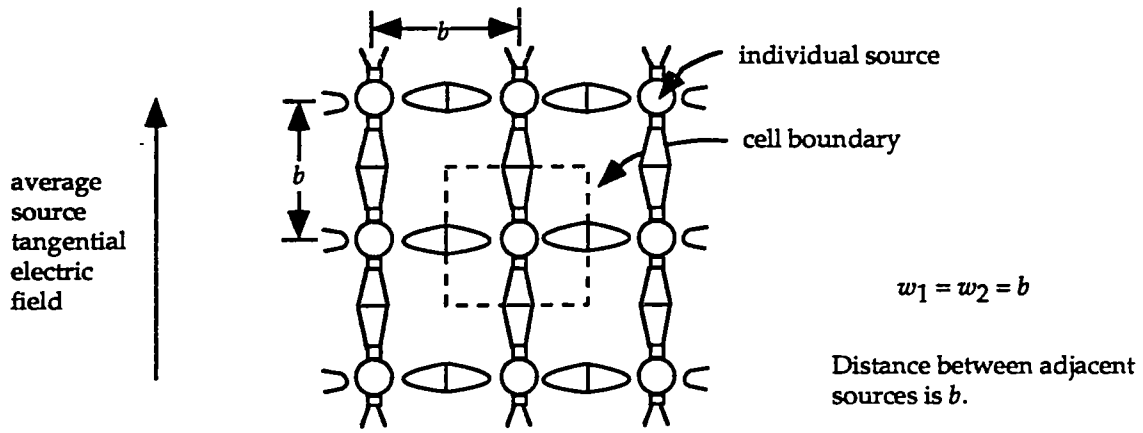
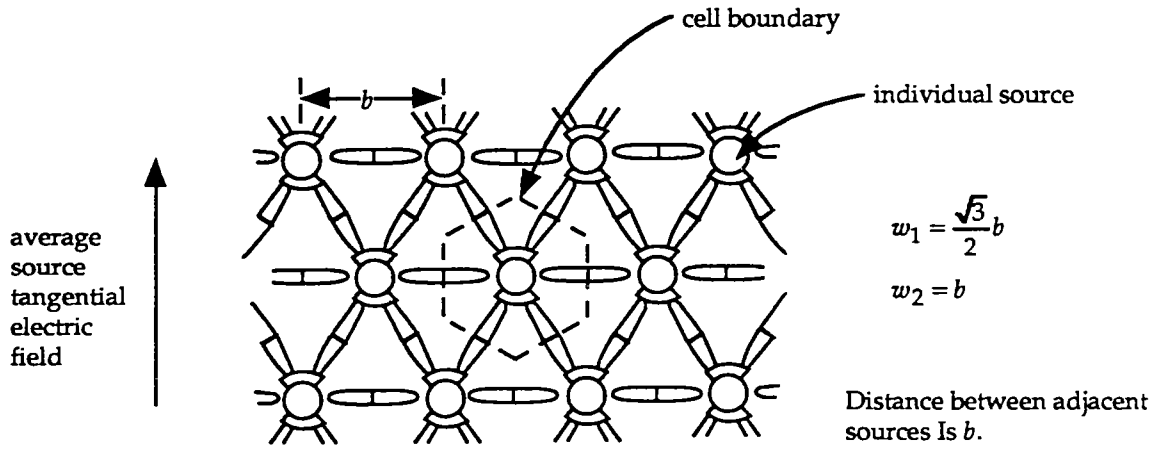


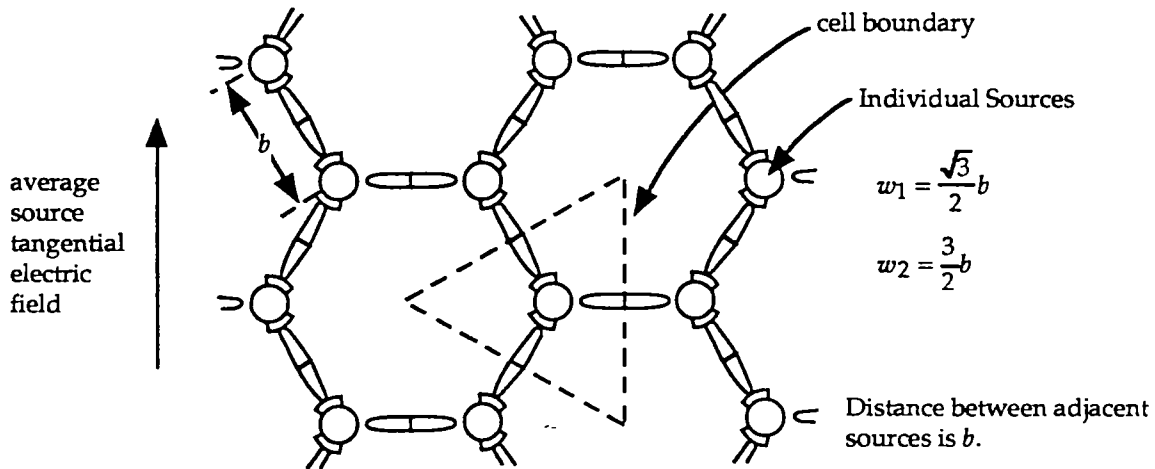
Fig. 3. Non-Planar Conical-Transmission-Line Array



A. Square Cell Geometry



B. Regular Hexagonal Cell Geometry



C. Equilateral triangular Cell Geometry

Fig. 4. Arrays for Changing Polarization: Top Views

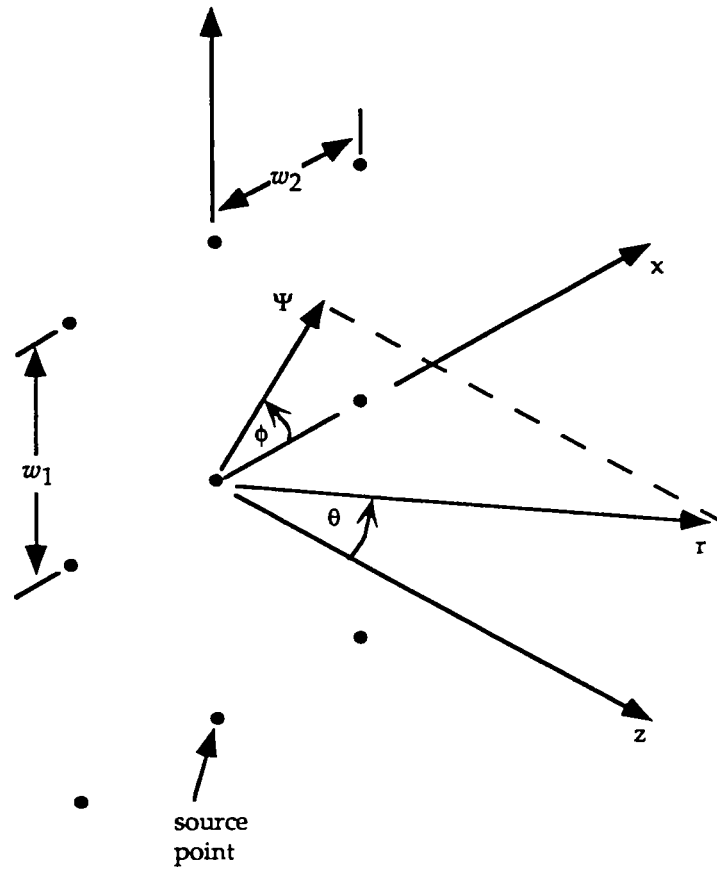


Fig. 5. Rectangular Array of Spherical TEM Elements

As one would expect as one makes the length ℓ of the conical transmission line larger than the opening w_1 (plate separation at the aperture plane where the individual plates connect to adjacent ones) the field at some distance r continues to increase. On the center line (the z axis) we have

$$\vec{F}(\theta=0, \phi) = \frac{\ell}{w_1} \vec{E}_{rel} \quad (2.2)$$

as the angle between the plates decreases, \vec{E}_{rel} being the electric field at the aperture plane on the z axis for 1 Volt between the plates (now approximately parallel). For wide plate ($w_2 \gg w_1$) $|\vec{E}_{rel}| \approx 1/w_1$. Note, however, that as ℓ/w_1 increases the time for which (2.1) is valid decreases due to the earlier arrival of the diffraction from the end of the conical plate (at the aperture plane). Furthermore, the behavior as in (2.1) being restricted to angles (θ, ϕ) lying between the plates (for far fields due to the presence of adjacent wave launchers), then large ℓ/w_1 (or ℓ/w_2) restricts θ to angles near 0, an important consideration in the context of array scanning.

Now, assuming an infinite array, we need to sum over the early-time signals of the individual elements. Let $\vec{1}_1$ define the direction propagation of a plane wave and define retarded time by

$$t_r \equiv t - \frac{\vec{1}_1 \cdot \vec{r}}{c}, \quad c = \text{speed of light} \quad (2.3)$$

The individual source points in the $z = 0$ plane are turned on (with $V_0 u(t_r)$) at zero retarded time at each source point. Then consider the field propagating in the $\vec{1}_1$ direction for large r with

$$\cos(\theta_1) = \vec{1}_1 \cdot \vec{1}_z > 0 \quad (2.4)$$

Restrict $\vec{1}_1$ (make θ_1 small enough) that (2.1) is valid for the individual elements for a window of retarded time

$$0 \leq t_r < t_{cf} \equiv \text{clear time in the far field (after which finite launcher dimensions can be observed)} \quad (2.5)$$

where t_{cf} is a function of (θ_1, ϕ_1) , being maximum (for symmetrical wave launchers) with $\theta_1 = 0$. By considering some t_r slightly greater than zero and letting $r \rightarrow \infty$ in the $\vec{1}_1$ direction more and more sources are seen by the observer. Summing these [11] over the expanding ellipse on the aperture plane (as $r \rightarrow \infty$) gives a far electric field for early times as

$$\vec{E}_{f0} = -\frac{2\pi V_0}{A_e \cos(\theta_1)} \vec{F}(\theta_1, \phi_1) ct_r u(t_r) \text{ for } t_r < t_{cf} \quad (2.6)$$

$A_e = w_1 w_2 \equiv \text{area of unit cell of array element}$

Note that in the limit the step has become a ramp function. This result applies to infinite arrays for which the far field does not decrease with r for constant retarded time. (This will be modified later for finite-size arrays.) The above result applies not only to rectangular arrays but other shapes in fig. 4 as well, with w_1 and w_2 appropriately interpreted.

The array performance can also be calculated for late times or low frequencies for which the wavelengths are large compared to element dimensions [11]. In this case one considers the average tangential electric field along the array as

$$\vec{E}_t = -\vec{1}_s \frac{V_0}{w_1} \quad (2.7)$$

where $\vec{1}_s$ can be considered as $\vec{1}_y$ in fig. 5 for convenience. Then with appropriate element symmetry [11] the late-time far field is (for step excitation)

$$\vec{E}_{f\infty} = \begin{cases} -\frac{V_0}{w_1 \cos(\theta_1)} \vec{1}_{\theta_1} \text{ in } E \text{ plane } (\phi_1 = \pi/2) \\ -\frac{V_0}{w_1} \vec{1}_y \text{ in } H \text{ plane } (\phi_1 = 0) \end{cases} \quad (2.8)$$

Equating this to the early-retarded-time result in (2.6), one can extrapolate the ramp to the late-time value to give an effective time constant for the rise of the far field as

$$ct_1 = \begin{cases} \left[\frac{\omega_2}{2\pi} \left| \vec{F}\left(\theta_1, \frac{\pi}{2}\right) \right| \right]^{-1} \text{ in } E \text{ plane} \\ \left[\frac{\omega_2}{2\pi} \left| \vec{F}(\theta_1, 0) \right| \cos(\theta_1) \right]^{-1} \text{ in } H \text{ plane} \end{cases} \quad (2.9)$$

For $t \gg w_1$ and w_2 , we can have t_1 arbitrarily small, except that θ_1 is restricted to smaller and smaller values.

Considering impedances, the value for early-time (high-frequency) considerations is tabulated for planar bicones [11], and is given by $Z_0/2$ for square unit cells (a self-complementary case) with $Z_0 \simeq 377 \Omega$ for free space. There are approximate values as well as more detailed calculations for non-planar flat-plate conical wave launchers [17]. For late times (low frequencies) the impedance appropriate to an individual unit cell is

$$Z_\ell = \begin{cases} \frac{Z_0}{2} \frac{w_1}{w_2} \cos(\theta_1) & \text{in } E \text{ plane} \\ \frac{Z_0}{2} \frac{w_1}{w_2} \cos^{-1}(\theta_1) & \text{in } E \text{ plane} \end{cases} \quad (2.10)$$

To minimize reflections, one can try to match early- and late-time results, but as these formulae indicate this is a function of $\frac{\ell}{w_1}$, albeit not a severe one if one restricts the variation of $\frac{\ell}{w_1}$ to not-too-large scan angles.

As ℓ/w_1 and ℓ/w_2 are increased ($\gg 1$) there is a significant interaction of the fields on an element with adjacent elements before the wave reaches the aperture plane. This can be partly accounted for by considering quasi TEM waves as on a multiconductor transmission line together with the symmetry conditions for a periodic structure. Allowing for this mutual coupling one can shape the wave-launching conductors to be no longer conical so as to optimize the wave transport to the aperture plane and the impedance presented to the sources. For the case of $\theta_1 = 0$ some analytic solutions have been obtained [18-21].

3. Modern Context

In applying these array concepts to even faster transient electromagnetic pulses (picoseconds for the fastest components) the first thing to observe is the usual electromagnetic scaling of time and frequency according to physical dimensions. The array elements basically need to be smaller, which for a given array size means many more elements. Of course, the switching for launching sufficiently fast-risetime pulses (with sufficiently small jitter) on the wave launchers needs to be incorporated as well.

Now we consider finite arrays. On the aperture plane (now $z = 0$) there is some electric field with tangential components $\vec{E}_t(\vec{r}_s, t)$ giving a far field [22, 29]

$$\vec{E}_f(\vec{r}, t) = \frac{1}{2\pi cr} \left[\vec{1}_z \cdot \vec{1}_r \vec{1} - \vec{1}_z \vec{1}_r \right] \cdot \frac{\partial}{\partial t} \int_{S_a} \vec{E}_t \left(\vec{r}'_s, t_r + \frac{\vec{1}_r \cdot \vec{r}'_s}{c} \right) dS' \quad (3.1)$$

$$\vec{1} \equiv \vec{1}_x \vec{1}_x + \vec{1}_y \vec{1}_y + \vec{1}_z \vec{1}_z \equiv \text{identity dyadic}$$

For the simple case that the observer is in the $\vec{1}_z$ direction (i.e., $\vec{1}_r = \vec{1}_z$) we have

$$\vec{E}_f(r \vec{1}_z, t) = \frac{1}{2\pi cr} \frac{\partial}{\partial t} \int_{S_a} \vec{E}_t(\vec{r}'_s, t_r) dS' \quad (3.2)$$

Furthermore, if we have a step-function tangential field on S_a (corresponding to a plane wave propagating in the $\vec{1}_1$ direction) we have

$$\vec{E}_t(\vec{r}_s, t) \equiv \vec{E}_{t0}(\vec{r}_s) u \left(t - \frac{\vec{1}_1 \cdot \vec{r}'_s}{c} \right) \quad (3.3)$$

$$\vec{E}_f(\vec{r}, t) = \frac{1}{2\pi cr} \left[\vec{1}_z \cdot \vec{1}_r \vec{1} - \vec{1}_z \vec{1}_r \right] \cdot \frac{\partial}{\partial t} \int_{S_a} \vec{E}_{t0}(\vec{r}'_s) u \left(t_r + \frac{\vec{1}_r \cdot \vec{r}'_s}{c} - \frac{\vec{1}_1 \cdot \vec{r}'_s}{c} \right) dS'$$

which on the beam center ($\vec{1}_r = \vec{1}_1$) reduces to

$$\begin{aligned}\vec{E}_f(r \vec{1}_1, t) &= \frac{1}{2\pi cr} \left[\vec{1}_z \cdot \vec{1}_r \vec{1} - \vec{1}_i \vec{1}_i \right] \cdot \delta_a(t_r) \int_{S_a} \vec{E}_{t_0}(\vec{r}'_s) dS' \\ \vec{E}_f(r \vec{1}_z, t) &= \frac{1}{2\pi cr} \delta_a(t_r) \int_{S_a} \vec{E}_{t_0}(\vec{r}'_s) dS' \text{ for } \vec{1}_1 = \vec{1}_z\end{aligned}\quad (3.4)$$

where δ_a is the approximate delta function [22]. Note the change in form from the infinite-array result. There is a $1/r$ dependence and the introduction of a time derivative in going from the near to the far field. The aperture S_a is assumed to be of finite linear dimensions with area A_a .

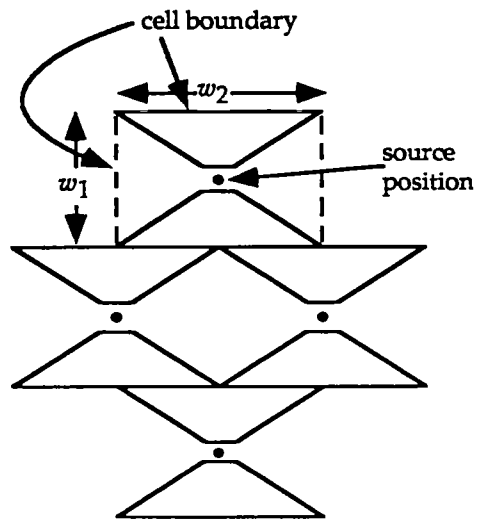
In applying the aperture integral to a transient array one can also see the effect of the field distribution on the unit cells for individual array elements. Instead of a simple plane-wave step excitation as in (3.3) one can view the actual aperture field as a deviation from this. Consider the simple case that the observer is in the $\vec{1}_z$ direction and all elements are turned on at the same time. If each element is a symmetrical conical transmission line of length ℓ , such as in the staggered cell arrangement in fig. 6, then, with a step-function TEM wave launched from the source, the wave does not arrive at the aperture plane all at the same time. There is a dispersion distance [1] or dispersion time which gives the difference in time of arrival of the field on each element unit cell of the aperture plane (for rectangular cells) as

$$\begin{aligned}d_e^{(1)} &\equiv ct_e^{(1)} \\ &= \left[\ell^2 + \frac{w_1^2 + w_2^2}{4} \right]^{\frac{1}{2}} - \ell \rightarrow \frac{w_1^2 + w_2^2}{8\ell} \text{ as } \frac{[w_1^2 + w_2^2]^{\frac{1}{2}}}{\ell} \rightarrow 0\end{aligned}\quad (3.5)$$

Using this in (3.2), then $t_e^{(1)}$ approximates the radiated pulse width due to the time derivative of the spatial integral of the field on the aperture plane. Note for large ℓ that $d_e^{(1)} \rightarrow 0$ for constant w_1, w_2 . However, as discussed previously, large ℓ also introduces significant coupling of the wave to adjacent cells before reaching the aperture plane, thereby modifying the fields that reach the aperture plane.

If, however, the array is to scan the beam over some angular domain of $\vec{1}_1$, then $t_e^{(1)}$ is not the only dispersion of interest for the unit cells [24]. As indicated in (3.3) the ideal field distribution on the aperture plane does not turn on all at once, but sweeps across the aperture, and hence across each unit cell in the array. The time difference in the ideal turn-on-time across the unit cell then gives another dispersion distance and time as

$$d_e^{(2)} = ct_e^{(2)} = w \sin(\theta_1) \quad (3.6)$$



Front View: Four unit cells shown

Fig. 6. Staggered Array of Flat-Plate Conical Wave Launchers in a Symmetrical Configuration

where w represents the width of the unit cell in the direction of wave propagation across the array. For the rectangular array, this can be w_1 and w_2 for particular directions, with $[w_1^2 + w_2^2]^{1/2}$ as the largest value achieved by w . If the individual element is designed to minimize $t_e^{(1)}$, there is still $t_e^{(2)}$ with which to reckon. This dispersion time also represents the pulse width in the far field so that $\delta_a(t_r)$ in (3.4) is replaced by a pulse of approximate width $t_e^{(2)}$, which we see increases with increasing θ_1 (by steering the beam off boresight).

One may combine these two dispersion times to obtain some effective total dispersion and effective far-field pulse width. If one limits θ_1 to some range $0 \leq \theta_1 \leq \theta_{1\max}$ centered on boresight, then $t_e^{(2)}$ is limited to some $t_{e\max}^{(2)}$. Looking again at $t_e^{(1)}$, there is not much point in making this too much smaller than $t_{e\max}^{(2)}$. So a certain consistency in design is called for in which these two time dispersions are roughly comparable.

As with the reflector [22] and lens [26] IRAs, an array IRA can also be designed to optimize its low-frequency performance [24]. As indicated in fig. 7, additional conductors can be added behind the array. The low-frequency (or late time) voltage across the array (summing the voltages of the series elements) induces a charge $+Q$ on the top conductors and $-Q$ on the bottom conductors thereby giving an electric-dipole moment \vec{p} for low frequencies. With an array of terminating resistors in the back, the low-frequency voltage produces a current I around a closed loop (including the source array), thereby giving a magnetic-dipole moment \vec{m} . With appropriate symmetry, these two moments are perpendicular and we have by proper choice of the termination resistors (controlling V/I)

$$\begin{aligned} \vec{p} &= p \vec{1}_y, \quad \vec{m} = -m \vec{1}_x, \quad p = \frac{m}{c} \\ \vec{p} \times \vec{m} &= p m \vec{1}_z \end{aligned} \tag{3.7}$$

This gives low-frequency directionality (a cardoid pattern) with maximum in the $\vec{1}_z$ direction (boresight) and a null in the $-\vec{1}_z$ direction. The example in fig. 7 is for a single polarization (the $\vec{1}_y$ direction with unit cells such as in fig. 3 or 6). One can also extend this low-frequency performance to the case of dual polarization [24] by the addition of conducting wires or strips (parallel to $\vec{1}_z$) on the sides as well as top and bottom. The termination resistors then form a two-dimensional grid in the back. The unit cells then take a form as in fig. 4A with two sources at each source point for the two orthogonal polarizations (or one source switched between the two orthogonal conical transmission lines).

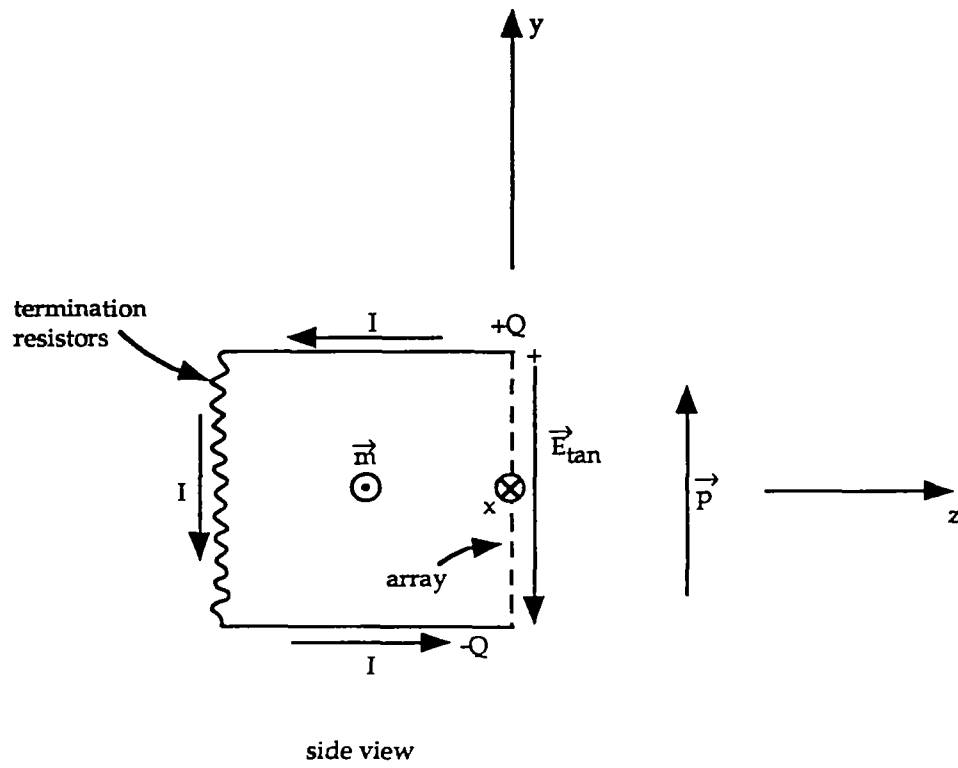


Fig. 7. Additions to Array for Balanced Low-Frequency Electric- and Magnetic-Dipole Moments

One can also apply the concept of self-complementary antennas to the design of transient arrays [25, 28]. In this case, not only the unit cells, but also the array as a whole (assumed infinite) is self complementary. This applies strictly only to planar arrays, but can apply approximately to non-planar arrays of planar bicones if ℓ is not very long; the characteristic impedance of the conical transmission line does vary much from the ideal value of $Z_0/2$ appropriate to square unit cells. The self-complementarity principle [31] is a symmetry in which the conducting sheets are replaced by free space, and conversely, and dyadic admittance sheets are replaced by other special sheets (the complement), but the structure remains the same except for a point symmetry operation (rotation, reflection), and now a translation as well. While this applies most simply to a square version of fig. 3 with square unit cells, other versions are possible with various types of impedance loading and other types of unit cells (e.g., as in fig. 4). The sources also enter into the consideration of self complementarity. The simplest case has identical sources, all triggered simultaneously so that $\vec{I}_1 = \vec{I}_z$ (boresight). These can be for a single polarization (as in fig. 3), or for two polarizations as in fig. 8 with two separate sets of sources with voltages $V^{(x)}$ and $V^{(y)}$ for the two polarizations [25, 28]. By including resistors of value $Z_0/2$ at these various connection points for sources one can retain self complementarity with sources that differ from each other (as in a scanning array) in the sense that an individual source (with all other sources zero) drives an impedance of $Z_0/2$ for all frequencies (or Z_0 if there is a $Z_0/2$ resistor with this source) [25]. However, when there is more than one source operating, one source does send currents through the other sources, so that one needs to allow for this.

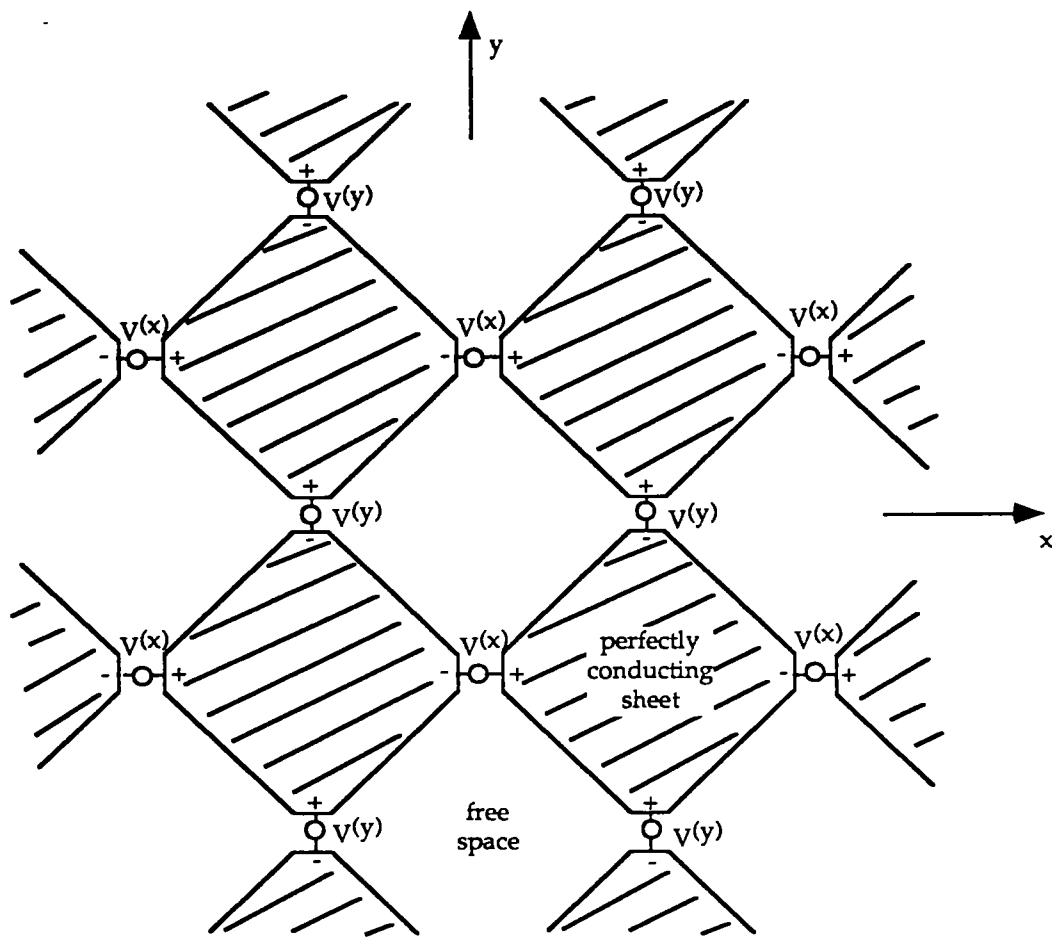


Fig. 8. Planar Array with C_{2ac} Symmetry and Dual Polarization

4. Concluding Remarks

Transient arrays can be designed to be impulse radiating antennas (IRAs) in a sense similar to reflector and lens IRAs for both high- and low-frequency performance. The array IRA is much more complicated than the other kinds due to the numerous array elements and associated timing requirements. However, one gains the ability to electronically scan. So it all depends on what function one wishes it to perform.

References

1. C. E. Baum, The Conical Transmission Line as a Wave Launcher and Terminator for a Cylindrical Transmission Line, *Sensor and Simulation Note 31*, January 1967.
2. G. W. Carlisle, Matching the Impedance of Multiple Transitions to a Parallel-Plate Transmission Line, *Sensor and Simulation Note 54*, April 1968.
3. C. E. Baum, The Distributed Source for Launching Spherical Waves, *Sensor and Simulation Note 84*, May 1969.
4. C. E. Baum, A Distributed-Source Conducting-Medium Simulator for Structures Near and Below the Ground Surface, *Sensor and Simulation Note 87*, July 1969.
5. C. E. Baum, Some Characteristics of Planar Distributed Sources for Radiating Transient Pulses, *Sensor and Simulation Note 100*, March 1970.
6. P. R. Barnes, Pulse Radiation by an Infinitely Long, Perfectly Conducting, Cylindrical Antenna in Free Space Excited by a Finite Cylindrical Distributed Source Specified by the Tangential Electric Field Associated with a Biconical Antenna, *Sensor and Simulation Note 110*, July 1970.
7. C. E. Baum, General Principles for the Design of ATLAS I and II, Part IV: Additional Considerations for the Design of Pulsar Arrays, *Sensor and Simulation Note 146*, March 1972.
8. C. E. Baum, General Principles for the Design of ATLAS I and II, Part V: Some Approximate Figures of Merit for Comparing the Waveforms Launched by Imperfect Pulsar Arrays onto TEM Transmission Lines, *Sensor and Simulation Note 148*, May 1972.
9. Z. L. Pine and F. M. Tesche, Pulse Radiation by an Infinite Cylindrical Antenna with a Source Gap with a Uniform Field, *Sensor and Simulation Note 159*, October 1972.
10. F. M. Tesche and Z. L. Pine, Approximation to a Biconical Source Feed on Linear EMP Simulators by Using N Discrete Voltage Gaps, *Sensor and Simulation Note 175*, May 1973.
11. C. E. Baum, Early Time Performance at Large Distances of Periodic Planar Arrays of Planar Bicones with Sources Triggered in a Plane-Wave Sequence, *Sensor and Simulation 184*, August 1973.
12. T. K. Liu, Admittances and Fields of a Planar Array with Sources Excited in a Plane Wave Sequence, *Sensor and Simulation Note 186*, October 1973.
13. C. E. Baum, EMP Simulators for Various Types of Nuclear EMP Environments: An Interim Categorization, *Sensor and Simulation Note 240*, January 1978, and *IEEE Trans. Antennas and Propagation*, 1978, pp. 35-53, and *IEEE Trans. EMC*, 1978, pp. 35-53.
14. C. E. Baum and D. V. Giri, The Distributed Switch for Launching Spherical Waves, *Sensor and Simulation Note 289*, August 1985.
15. Y.-G. Chen, S. Lloyd, R. Crumley, C. E. Baum, and D. V. Giri, Design Procedures for Arrays which Approximate a Distributed Source at the Air-Earth Interface, *Sensor and Simulation Note 292*, May 1986.

16. T. M. Flanagan, C. E. Mallon, R. Denson, R. Leadon, and C. E. Baum, A Wide-Bandwidth Electric-Field Sensor for Lossy Media, *Sensor and Simulation Note 297*, January 1987.
17. D. V. Giri and C. E. Baum, Early Time Performance at Large Distances of Periodic Arrays of Flat-Plate Conical Wave Launchers, *Sensor and Simulation Note 299*, April 1987.
18. C. E. Baum, Coupled Transmission-Line Model of Period Array of Wave Launchers, *Sensor and Simulation Note 313*, December 1988.
19. D. V. Giri, Impedance Matrix Characterization of an Incremental Length of a Periodic Array of Wave Launchers, *Sensor and Simulation Note 316*, April 1989.
20. C. E. Baum, Canonical Examples for High-Frequency Propagation on Unit Cell of Wave-Launcher Array, *Sensor and Simulation Note 317*, April 1989.
21. D. V. Giri, A Family of Canonical Examples for High Frequency Propagation on Unit Cell of Wave-Launcher Array, *Sensor and Simulation Note 318*, June 1989.
22. C. E. Baum, Radiation of Impulse-Like Transient Fields, *Sensor and Simulation Note 321*, November 1989.
23. Y.-G. Chen, S. Lloyd, and R. Crumley, Low Voltage Experiments Concerning a Section of a Pulsed Array Near the Air-Earth Interface, *Sensor and Simulation Note 322*, February 1990.
24. C. E. Baum, Timed Arrays for Radiating Impulse-Like Transient Fields, *Sensor and Simulation Note 361*, July 1993, and *Proc. SPIE Automatic Object Recognition V*, Orlando Florida, April 1995, Vol. 2485, pp. 168-174.
25. C. E. Baum, Self-Complementary Array Antennas, *Sensor and Simulation Note 374*, October 1994.
26. C. E. Baum, Low-Frequency-Compensated TEM Horn, *Sensor and Simulation Note 377*, January 1995.
27. C. E. Baum, From the Electromagnetic Pulse to High-Power Electromagnetics, *System Design and Assessment Note 32*, June 1992, and *Proc. IEEE*, 1992, pp. 789-817.
28. N. Inagaki, Y. Isogai, and Y. Mushiake, Self-Complementary Antenna with Periodic Feeding Points, *Trans. IECE*, Vol. 62-B, No. 4, 1979, pp. 388-395, in Japanese. Translation NAIC-ID(RS)T-0506-95, 11 December 1995, National Air Intelligence Center.
29. C. E. Baum and E. G. Farr, Impulse Radiating Antennas, pp. 139-147, in H. Bertoni et al (eds.) *Ultra-Wideband, Short-Pulse Electromagnetics*, Plenum Press, 1993.
30. E. G. Farr, C. E. Baum, and C. J. Buchenauer, Impulse Radiating Antennas, Part II, pp. 159-170 in L. Carin and L. B. Felsen (eds.), *Ultra-Wideband, Short-Pulse Electromagnetics 2*, Plenum Press, 1995.
31. C. E. Baum and H. N. Kritikos, Symmetry in Electromagnetics, ch. 1, pp. 1-90, in C. E. Baum and H. N. Kritikos (eds.), *Electromagnetic Symmetry*, Taylor & Francis, 1995.